Landsc Ecol
https://doi.org/10.1007/s10980-023-01646-6

RESEARCH ARTICLE

Improved topographic ruggedness indices more accurately model fine-scale ecological patterns

Thomas E. Dilts · Marcus E. Blum · Kevin T. Shoemaker · Peter J. Weisberg · Kelley M. Stewart

Received: 27 May 2022 / Accepted: 26 March 2023

Abstract
Context Topographic ruggedness has been examined in thousands of ecological studies and is a popular variable for characterizing habitat selection. Despite widespread adoption, ruggedness metrics are often applied uncritically and require systematic and thorough testing using both artificial landscapes and real-world applications.
Objectives In this paper we introduce a technique that removes the correlation of topographic ruggedness with curvature in order to more accurately represent fine-scale surface ruggedness.
Methods We test our modified version of several ruggedness metrics against traditional ruggedness metrics using three ideal ruggedness criteria in artificial landscapes. We further tested our modified ruggedness measures using 449 real mountain ranges in Nevada, USA. Using desert bighorn sheep as a case study, we tested both modified and uncorrected ruggedness measures and slope in a multiscale context in order to examine habitat selection by female bighorn sheep.
Results The modified versions of the metrics passed all three criteria of the ideal ruggedness test and was able to accurately capture surface ruggedness. Modified versions of ruggedness differed from uncorrected versions by containing fewer highly rugged cells along ridgelines and drainages. Habitat relationships of desert bighorn sheep with ruggedness were scale-dependent, such that female sheep selected for steep slopes at fine spatial scales and ruggedness at moderate spatial scales.
Conclusions We demonstrate that there are three components to ruggedness: elevation variation, aspect diversity, and surface ruggedness representing first, second, and third generation ruggedness indices. Our technique for removing underlying topographic variation provides an improved mapping of surface ruggedness and augments the other two generations of ruggedness metrics.

Keywords Ruggedness · Topography · Roughness · Gradient · Bighorn sheep · Habitat selection

Supplementary Information The online version contains supplementary material available at https://doi.org/10.1007/s10980-023-01646-6.

T. E. Dilts (✉) · M. E. Blum · K. T. Shoemaker · P. J. Weisberg · K. M. Stewart
Department of Natural Resources and Environmental Science, University of Nevada, 1664 N Virginia Street, Reno, NV 89557, USA
e-mail: tdilts@unr.edu

Introduction

Spatial heterogeneity is central to the field of landscape ecology and is an important determinant for many ecological processes including soil development, movement of water and nutrients through ecosystems, microclimates, and disturbance on landscapes (Pickett & Cadenasso 1995). These ecological processes give way to the diverse biota and further modify the mobility of organisms across the landscape (Wiens et al. 1993). Topography has long been considered to be one of the central drivers of spatial heterogeneity (Li & Reynolds 1995). The most common representation of topographic surfaces are digital elevation models, which are gridded elevation maps in raster form, and are widely used in ecological modeling. Digital elevation models are used to construct a wide variety of topographic derivatives, such as slope, aspect, and topographic ruggedness maps (Amatulli et al. 2018). Elevation derivatives are used to understand both direct controls on species distributions (Austin 2002) and indirect controls that are expressed through climate and microclimate (Leempoel et al. 2015). Many of the higher-order measures of ruggedness have been developed independently through time and are calculated in a myriad of ways, which leads to a lack of guidance and potential confusion. In many instances, metrics of the same name may have very different meanings. Topographic ruggedness is one such measure having seen development from both inside (Sappington et al. 2007) and outside of the field of ecology (Melton 1958).

Topographic ruggedness (alternatively, known as surface roughness, rugosity, terrain complexity) is often defined as “the deviations in the direction of the normal vector of a real surface from its ideal or intended form” (Whitehouse 1994). In ecology, indices of topographic ruggedness are typically used to measure microhabitat diversity, difficulty of movement, the ability of a habitat to provide shelter from extreme weather conditions, or escape from predators. Numerous studies have confirmed the utility of topographic ruggedness metrics in assessing habitat quality for a wide array of animal and plant species. For example, research on wild sheep has consistently shown that areas of high topographic complexity are critical for predator avoidance, especially around parturition (McCann 1956; Buechner 1960; Johnson et al. 2013; Hoglander et al. 2015; Smith et al. 2015; Bleyl et al. 2019). Similarly, many studies of predator ecology have shown strong relationships in selection (felids) or avoidance (canids) of topographic ruggedness (Chetkiewicz & Boyce 2009; Kunkel et al. 2013; Lone et al. 2014). In marine environments, complex surfaces, such as coral reefs, create escape terrain from predators making them amongst the most productive and diverse ecosystems in the world (Rengstorf et al. 2013; Graham and Nash 2013). In the riverine environment roughness of the river bed as well as roughness created by coarse woody debris creates areas with low velocity of flow, which allow fish to rest, replenish their energy and food stores, and move upstream (Buffington et al. 2004).

Topographic heterogeneity has been shown to be an important driver of local microclimates (Dobrowksi et al. 2009), which have been linked with higher species diversity of plants (Copeland et al. 2015). Topographic ruggedness can also influence the frequency and spread of disturbances. For example, Krawchuk et al. (2016). found that topographic ruggedness was an important determinant for whether a site was likely to become a fire refugium or not. Ruggedness can also influence the movement of animal species leading to differences in herbivory through time. For example, Seidl and Boyce (2015) found that ruggedness was an important variable in determining which habitat patches were grazed by elk. Similarly, Heffelfinger et al. (2020) found that mule deer grazing was higher in low ruggedness areas compared to high ruggedness areas. Donadio and Buskirk (2016) found that topographic ruggedness increased the efficiency of puma kills on vicuñas, which also resulted in differences in primary productivity.

Generally speaking, indices of topographic ruggedness (Fig. 1) can be classified into two generations (see also Appendix S1). The first generation of indices are those that are correlated with slope making it impossible to disentangle the ecological differences that may be related to slope versus those related to ruggedness per se (Strahler 1954; Melton 1958; Beasom 1983; Hobson et al. 1972; Nelleman and Thomsen 1994; Riley et al. 1999; Jenness 2004). Sappington et al. (2007), and later Du Preez (2015), recognized this limitation and created the Vector Ruggedness Measure (VRM) and Arc-Chord Ratio (ACR) respectively to minimize this correlation. Those improvements allowed ecologists and others to separate the effects of ruggedness from that of slope, which lead to better statistical predictions and better habitat models. The use of topographic ruggedness indices in ecology has increased dramatically through time with the advent of Geographic Information Systems and modern habitat modeling techniques among the most likely drivers of this increase in use.

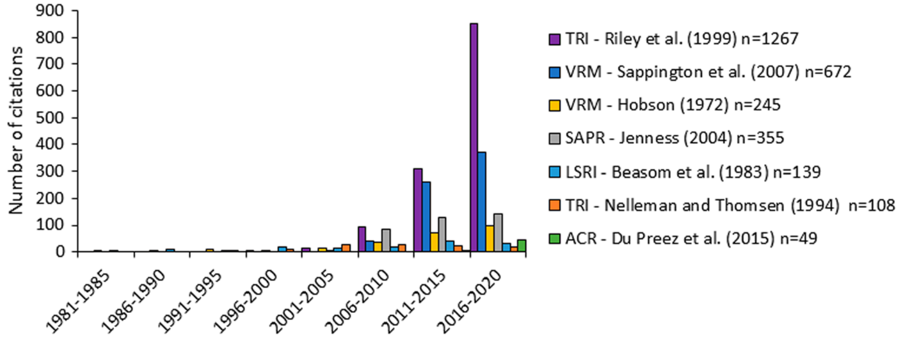

Fig. 1 Literature review of major ruggedness indices used in ecology based on a Google Scholar search. LSRI = land surface ruggedness index. TRI = Terrain Ruggedness Index. SAPR = Surface-area Planar-area Ratio. VRM = Vector Ruggedness Measure. ACR = Arc-chord Ratio

Despite the advantages of second generation ruggedness indices, such as VRM and ACR, however those methods still suffer from inflated ruggedness values in folded, yet smooth, landscapes. Areas such as ridgelines and drainages, in particular, tend to have very high values of VRM and ACR, because they contain adjacent cells that face different directions resulting in high ruggedness values despite representing what would appear to be smooth from a human perspective. This issue is problematic because ridgelines and drainages may provide habitat features or affect physical processes in ways that are independent of topographic ruggedness (Fig. 2). For example, ridgelines have been found to be associated with higher levels of lightning strikes (Yang et al. 2015), snow drifts (Baker and Weisberg 1995), and greater visibility (MacDonald et al. 2018), whereas drainages may be associated with higher levels of water and nutrient accumulation (Burt and Butcher 1985), and possibly animal movement pathways (Monteith et al. 2018). Hence, developing ruggedness metrics that also remove the correlation with curvature are important for distinguishing between smooth folded terrain and truly rugged terrain.

An ideal ruggedness index should have a minimum of three distinct properties. First, it should be independent of slope to allow the researcher to examine the effects of slope and ruggedness separately. Second, it should not be influenced by smooth folding, such as occurs on ridgelines and drainages that have high values simply because they contain different slope-aspects within a neighborhood. Finally, an ideal ruggedness metric should respond positively to distortion in the z dimension for non-smooth surfaces. The primary goal of this paper is to develop and test a method for calculating topographic ruggedness that alleviates the confusion between rugged areas and ridgelines and drainages. This index meets all three criteria for being an "ideal" ruggedness index, which constitutes what we consider to be a third generation of topographic ruggedness indices. Furthermore, we have applied this method to a specific landscape to better understand the role of ruggedness in defining habitat for desert bighorn sheep, and the scale(s) at which those ungulates respond to the ruggedness of their environment. Desert bighorn sheep are an excellent case study for looking at indices of terrain ruggedness because habitat selection has been shown to be driven by topographic ruggedness (Sappington et al. 2007), especially for females with dependent young.

In this paper, we ask the following questions: (1) Do the newly-developed metrics, such as VRML, ACRL, and SAPRL, as well as the established VRM, ACR, and SAPR, meet the criteria of an "ideal" ruggedness index? (2) Does VRML result in fewer highly rugged cells located in ridgelines and drainages compared to VRM across the 494 mountain ranges in Nevada? Using desert bighorn sheep at Lone Mountain, Nevada, USA as a case study, we investigated several questions related to habitat selection by female bighorn sheep, both with and without dependent young. Finally (3), we asked the question: Which habitat features and spatial scales are most important for female bighorn sheep with young compared to females without young?

Methods

Overview

In this study we evaluated three measures of surface ruggedness commonly used in ecology: surface-area

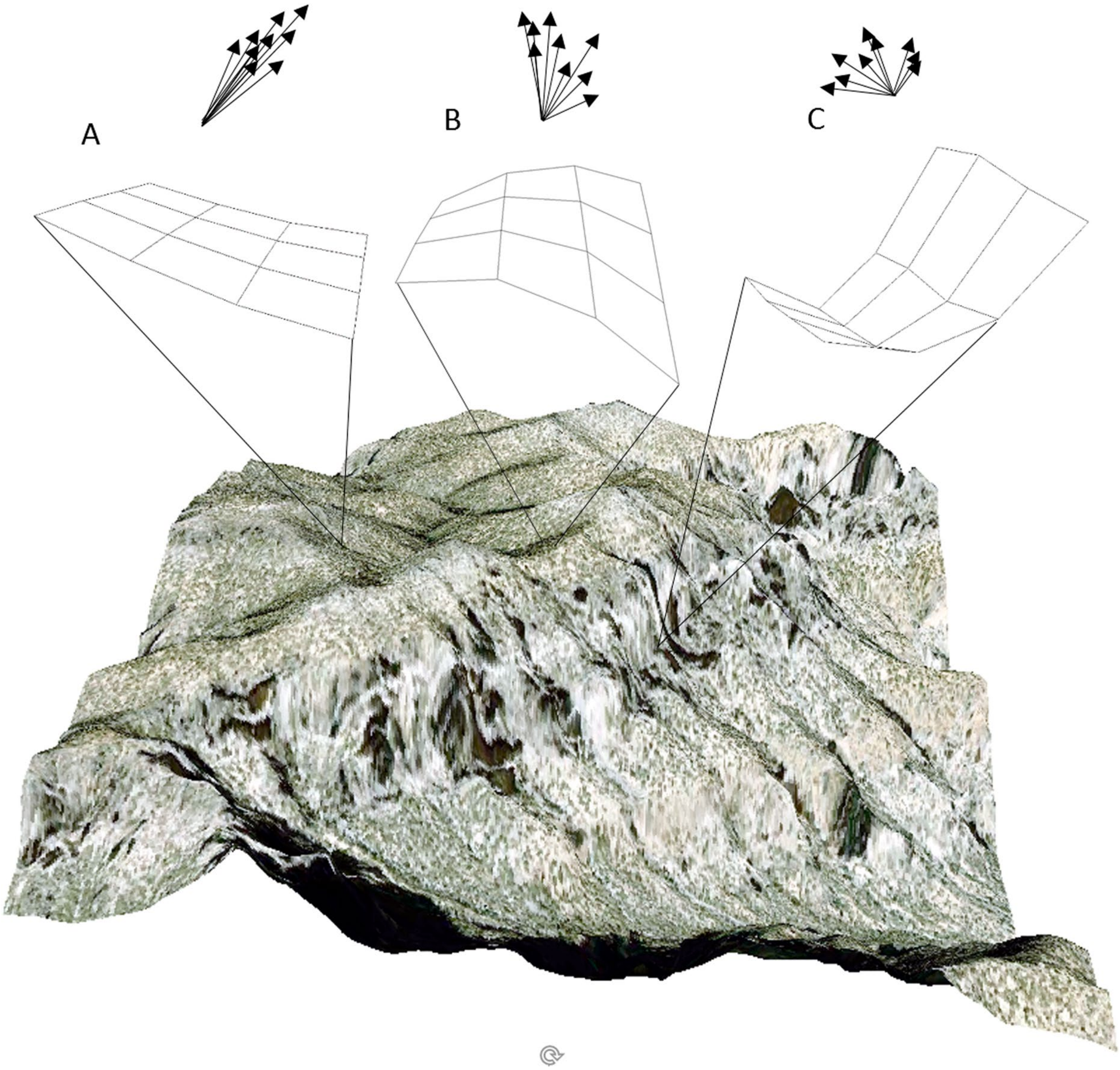

Fig. 2 Three-dimensional representation of mountainous topography illustrating how the Vector Ruggedness Measure (VRM) may result in large values along ridgelines and drainages because aspects differ strongly at ridgelines and drainages despite the fact that underlying topographic variation can be smooth. **A** Gentle slopes with similar aspects have a VRM of 931. **B** Gentle slopes along a ridgeline have a VRM value of 2453 because of the strong contrast between east and west aspects. **C** Steep cliffband with differing aspects has a VRM of 4173. The difference in VRM between the ridgeline and cliff and the ridgeline and gentle slope are similar. Location is 36.831° N, 115.105° W in the Sheep Range in southern Nevada

to planar-area ratio (SAPR, Jenness 2004), vector ruggedness measure (Hobson 1972; Sappington et al. 2007), and the arc-chord ratio (Du Preez 2015), and then modify these three metrics using a simple pre-processing technique that removes the underlying smooth topography. Our approach to modifying SAPR, ACR, and VRM is conceptually simple. We first apply a smoothing function such as a 3 × 3 neighborhood mean (Lindsay and Newman 2018) and then subtract the original DEM surface from the underlying smooth surface in order to remove overall trend in topographic gradient and create a raster that only contains the surface variation. Next, we calculate the original ruggedness measures, such as SAPR, VRM, and ACR using this raster of surface variation with the underlying smooth topography removed. We denote these modified indices as SAPRL, VRML, ACRL where L stands for local.

Testing the metrics using the ideal ruggedness test with artificial landscapes

We designed six levels of artificial landscapes to assess topographic ruggedness indices using the three ideal ruggedness criteria resulting in eighteen artificial landscapes. The first criterion was that topographic ruggedness should be orthogonal to slope. We tested this criterion by comparing each ruggedness index with a set of smooth, planar landscapes that differed only by slope; under the first criterion, topographic ruggedness should remain at zero regardless of slope. The second criterion was that topographic peaks and valleys (and other curvatures or folds) should not automatically be identified as “rugged” terrain – just as a quadratic curve or sine wave should be considered equally smooth across its range of support. We tested this criterion by confronting each topographic ruggedness index with a set of smooth artificial landscapes that were folded according to sine waves with varying frequency (i.e., generating smooth landscapes that differed only by ‘foldedness’). Topographic ruggedness should remain at zero regardless of the number of folds, assuming the scale of the folds is much larger (e.g., peaks and valleys occurring > 10 grid cells apart) than the raster resolution. Finally, we applied a third test by generating a random raster and increased vertical distortion by multiplying the raster by values of 2, 4, 8, 16, and 32. All measures of ruggedness should increase with increasing vertical distortion regardless of slope or foldedness.

Comparison of VRM and VRML across 494 mountain ranges in the state of Nevada

To compare how the modified versions of the ruggedness indices in which the smooth underlying topographic variation has been removed compared to the uncorrected version we calculated VRM and VRML across the 494 mountain ranges that occur within the state of Nevada. The mountain ranges in the state of Nevada are a good case study for this comparison because they provide numerous replicates and, because of the basin and range topography in which mountains alternate with valleys, the boundaries of these ranges tend to be distinct from one another. We chose to compare VRM because it is the most widely used 2nd generation ruggedness index in ecology (Sappington et al. 2007 has been cited 541 times compared with Du Preez (2015), which has been cited 32 times). All calculations were performed on 1/3 arc-second digital elevation models (DEMs) derived from the USGS (2009). To create VRML we prepared the DEMs by running a 3×3 neighborhood mean on each original DEM to create a smoothed DEM and then subtracting the smoothed DEM from the original DEM to create a local difference DEM. Next, we used the Benthic Terrain Modeler Version 3.0 Toolbox for ArcGIS (Walbridge et al. 2018) and calculated the vector ruggedness measure (Eq. 2) on the original un-processed DEM and local difference VRM using the rugosity tool. To summarize average VRM and VRML we calculated the average value within polygons from a hand-digitized shapefile of mountain ranges in the state of Nevada (Robert Elston Jr. pers. comm.). Finally, we compared the residuals of a linear regression of VRML on VRM in order to determine the characteristics for mountain ranges that varied the most between VRM and VRML.

To determine whether VRML led to a reduction in the area classified as rugged ridgelines and rugged drainages compared to mid-slope we divided the landscape into each of the three topographic position categories using the Topographic Position Index of Weiss (2001). We used the same 1/3 arc-second digital elevation model as in previous steps and calculated the Topographic Position Index using a 450 m neighborhood size using the entire state of Nevada. Cells with the highest 10% of TPI values were classified as ridgelines and cells with the lowest 10% of TPI values were classified as drainages. All remaining cells were classified as midslopes. To identify the most rugged cells we then took the top 10% of VRM and VRML within Nevada mountain ranges and classified them as rugged, overlaid them with the three topographic position categories, and calculated the proportion of rugged cells in each topographic position category.

Habitat selection by desert bighorn sheep during the parturition season

We tested the modified and uncorrected versions of three ruggedness metrics (SAPR, ACR, VRM) in combination with slope angle across a range of spatial scales for desert bighorn sheep (*Ovis canadensis nelsoni*) at Lone Mountain, Nevada. Using radio-collar data from 30 individuals we tested selection for topographic ruggedness and slope angle on Lone Mountain (38° 2′ N 117° 31′ W) during parturition (birthing and 1 month following birth) in 2016–2018. Lone Mountain is an extremely steep and rugged mountain, has an average slope of 15.3°, and represents one of the last remnant genetic populations of desert bighorn sheep in the Great Basin (Jahner et al. 2019). Hence, desert bighorn sheep and the population at Lone Mountain, in particular, make an excellent case study for examining habitat selection using the newly developed and original ruggedness indices. Additionally, we included slope as a variable because slope and ruggedness may represent different physical properties of the landscape that are important for female bighorn sheep with and without dependent young.

In 2016–2018 we captured seventeen female desert bighorn sheep on Lone Mountain. We used ultrasonography to determine pregnancy status of each captured individual (Bishop et al. 2007). Pregnant individuals were fit with GPS collars (Vertex Plus Iridium, Vectronic Aerospace, Berlin, Germany), and a vaginal implant transmitter (VITs) was inserted into the birth canal of each pregnant female. Following capture, individuals were monitored via radio telemetry for parturition events. Following confirmed parturition events, researchers attempted to capture and collar dependent young with very high frequency (VHF) expandable collars. Dependent young were then monitored for survival during the ensuing months and mortalities were investigated to determine cause. All handling of animals was approved by the Institutional Animal Care and Use Committee (University of Nevada, Reno IACUC Protocol 00651).

Following each field season, we subset the GPS location data to the 1st month following parturition of individuals that were provisioning a neonate. We chose this period because females selected differing degrees of slopes and ruggedness to increase survival of young during the 1st month of life (Blum et al. 2023b). We buffered those locations by 780 m and dissolved all buffers into a single polygon to generate the availability boundary to be used in habitat selection functions. We selected those distances by measuring the movement rate between each GPS location, per individual, and estimating the distance that 99% of locations fell within (standard deviation * 2.58) based on those movement rates. Furthermore, we subset the location dataset to include a maximum of 2 locations per day (i.e., one in the morning and one in the evening) to reduce spatial autocorrelation in the dataset. We created two random locations for every used location (i.e. each sheep GPS location in the dataset) within the buffered polygon.

We generated slope and ruggedness metrics at twenty-one spatial scales. Understanding the interactions between slope and ruggedness for species such as bighorn sheep is best examined in a multiscale framework, because selection for one variable may occur at spatial scale very different from the other. A majority of ruggedness measures in the ecological literature, including VRM, ACR, and SAPR, are scale-dependent and require the investigator to explicitly define the scale at which to calculate the measure. Multiscale habitat modeling has become more widespread as a tool for discovering the relevant spatial scales for organisms (McGarigal et al. 2016). For each study area we used 1/3 arc-second DEM and created slope and ruggedness rasters at 21 spatial scales. To calculate slope we used Spatial Analyst in ArcGIS, and to calculate SAPR, ACR, and VRM using the Benthic Terrain Modeler Version 3.0 Toolbox for ArcGIS (Walbridge et al. 2018) and calculated each ruggedness measure at each spatial scale. For the modified version of each ruggedness measure we first prepared the DEM by running a 3×3 neighborhood mean on each original DEM to create a smoothed DEM and then subtracting the smoothed DEM from the original DEM to create a local difference DEM. We then calculated SAPRL, ACRL, and VRML using the local difference DEM. We extracted values from each covariate (SAPR, SAPRL, ACR, ACRL, VRM, and VRML) to the used and random locations. We used logistic regression models, to determine which ruggedness metrics were most effective in predicting bighorn sheep habitat selection. We generated these models through the "lme4" package in R 3.6.1 (Manly et al. 2002; Johnson et al. 2006; Bates et al.

2015). We set used and random locations as the binary response variable and the slope and ruggedness covariates to predictor variables. We generated a model for every combination of slope and ruggedness, across the 21 spatial scales (n = 2,646 models). Each model contained two predictor variables, a slope and ruggedness metric (e.g. slope*ACR), that were set as an interaction, so that we could estimate additive and interaction effects for each spatial and variable combination. We evaluated each of the logistic regression models using the McFadden's R2 (McFadden 1974) and by assessing the additive ruggedness and slope coefficients for all models.

We expected females with young under 1 month of age to select for high ruggedness and steep slopes, referred to as risk-averse selection of habitat because females provisioning young frequently give up forage resources in exchange for predator avoidance (Blum 2023a). We divided our GPS locations into two groups: pre-parturition which included locations < 2 months prior to birth and post-parturition which included locations 1 month after birth. We selected optimized scales of ruggedness (VRML) and slope based on the previous multi-scale logistic regression analysis. In addition to localized terrain ruggedness, we generated and appended elevation, slope, sin of aspect, and cosine of aspect to GPS locations. Additionally, we calculated distance to water from perennial water sources on Lone Mountain. We used the Rangeland Analysis Platform to append vegetation cover to each location (Jones et al. 2018). Our vegetation cover classes included cover of annual forbs and grasses, perennial forbs and grasses, shrubs, trees, and bare ground.

Prior to analyses of habitat selection, we tested for multicollinearity among variables. Each localized terrain ruggedness variable had high correlation with the others (i.e., > 0.6), therefore we conducted six logistic regressions, with each ruggedness variable as a single predictor variable, to determine which variable had the most predictive power. We selected VRML as the ruggedness metric for our habitat selection functions, because it had the lowest AICc score. Furthermore, we standardized all predictor variables so that selection coefficients could be directly compared.

We modeled habitat selection of bighorn sheep pre and post parturition through a Bayesian hierarchical framework. We generated a separate model for each parturition period and compared the selection coefficients from each model. We used the "jagsUI" package in R to fit each model (Kellner 2019). We modeled used and random location of individual female sheep, n, for each day, j, and observation, k, using a Bernoulli distribution and estimated the relative probability of using that location, pi,j,k, as a logit linear function of our covariates, Xn:

$$y_{i,j,k} \sim Bernoulli(p_{i,j,k}) \tag{1}$$

$$\mathrm{logit}(p_{i,j,k}) = \beta_0 + \beta_{1,i,j} X_{1,i,j,k} \dots \beta_{n,i,j} X_{n,i,j,k} \tag{2}$$

We used vague prior distributions for all estimated parameters. We tested all model iterations for convergence using Rhat scores and by visually analyzing MCMC chain mixture. We used 20,000 iterations, with a burn in of 1000 iterations, and 3 MCMC chains to get models to converge.

Results

Artificial landscapes

Our results show that the measures of topographic ruggedness responded differently to each of the three landscape properties: increasing vertical distortion, increasing slope of a plane, and increasing frequency of a smooth wave (Table 1). Only the modified versions of those measures, in which underlying smooth topography was minimized, passed all three tests. The original surface area to planar area ratio (SAPR) failed both the slope and the smooth wave tests indicating that it was influenced by 1st order slope influences and 2nd order curvature influences. The uncorrected versions of the arc-chord ratio (ACR) and vector ruggedness measure (VRM) both passed the slope test, but failed the smooth wave test. Those results indicated that they were successful in reducing the correlation with slope, but failed to successfully reduce the correlation with curvature. In contrast, all three modified versions of the ruggedness metrics (SAPRL, ACRL, and VRML), with smooth underlying topographic variation removed, passed all three tests suggesting that they were not influenced by topographic folding.

Table 1 Mean ruggedness for each artificial landscape test

(a) ruggedness must increase with vertical distortion						
Vertical distortion	SAPR	ACR	VRM	$SAPR_L$	ACR_L	VRM_L
1	1.0016	1.0015	0.0001	1.0012	1.0012	0.0000
2	1.0066	1.0059	0.0005	1.0048	1.0045	0.0003
4	1.0258	1.0233	0.0021	1.0190	1.0178	0.0011
8	1.0976	1.0870	0.0083	1.0728	1.0676	0.0045
16	1.3338	1.2857	0.0307	1.2557	1.2324	0.0175
32	1.9821	1.7533	0.0981	1.7788	1.6631	0.0613
Polynomial	3rd	3rd	3rd	3rd	3rd	3rd
Passed?	Yes	Yes	Yes	Yes	Yes	Yes
Generation	1st	2nd	2nd	3rd	3rd	3rd
(b) ruggedness must not increase with increasing slope						
Planar slope (degrees)	SAPR	ACR	VRM	$SAPR_L$	ACR_L	VRM_L
0.000000	1.0000	1.0000	0.0000	1.0000	1.0000	0.0000
0.045293	1.0000	1.0000	0.0000	1.0000	1.0000	0.0000
0.090586	1.0000	1.0000	0.0000	1.0000	1.0000	0.0000
0.181173	1.0000	1.0000	0.0000	1.0000	1.0000	0.0000
0.362339	1.0000	1.0000	0.0000	1.2557	1.2324	0.0175
0.724650	1.0001	1.0000	0.0000	1.7788	1.6631	0.0613
Polynomial	2nd					
Passed?	No	Yes	Yes	Yes	Yes	Yes
(c) ruggedness must not increase with increases folding						
Sine wave (frequency)	SAPR	ACR	VRM	$SAPR_L$	ACR_L	VRM_L
1	1.0000	1.0000	0.0000	1.0000	1.0000	0.0000
2	1.0000	1.0000	0.0000	1.0000	1.0000	0.0000
4	1.0000	1.0000	0.0000	1.0000	1.0000	0.0000
8	1.0001	1.0000	0.0000	1.0000	1.0000	0.0000
16	1.0004	1.0000	0.0000	1.0000	1.0000	0.0000
32	1.0015	1.0002	0.0005	1.0000	1.0000	0.0000
Polynomial	2nd	3rd	3rd			
Passed?	No	No	No	Yes	Yes	Yes

SAPR surface area to planar area ratio, ACR Arc-chord ratio, and VRM vector ruggedness measure. L in subscript denotes the modified (local) version of each of these measures. Univariate regressions were developed between each landscape property (first column) and the mean ruggedness derived from each measure. The bottom rows indicates the best-fit polynomial, whether the test was passed, and the generation that the ruggedness index belongs to. In cases where there was no first, second, or third order polynomial we concluded that no simple relationship existed between the landscape property and the ruggedness measure tested. The three tests were (a) ruggedness must increase with vertical distortion in the z dimension, (b) ruggedness must not increase with increasing slope, and (c) ruggedness must not increase with increases folding as measured by the number of sine waves.

Comparison of VRM and VRM_L across mountain ranges

VRM and VRML were strongly related to one another (R2 = 0.76; Fig. 3) yet there were important differences with mountain ranges above the regression line exhibiting characteristics that are classically thought of as rugged, such as steep cliff bands and extensive rock outcrops. Whereas mountain ranges below the regression line contained fewer rock outcrops and had smoother topography despite having steep slopes and a variety of aspects. In general, the majority of

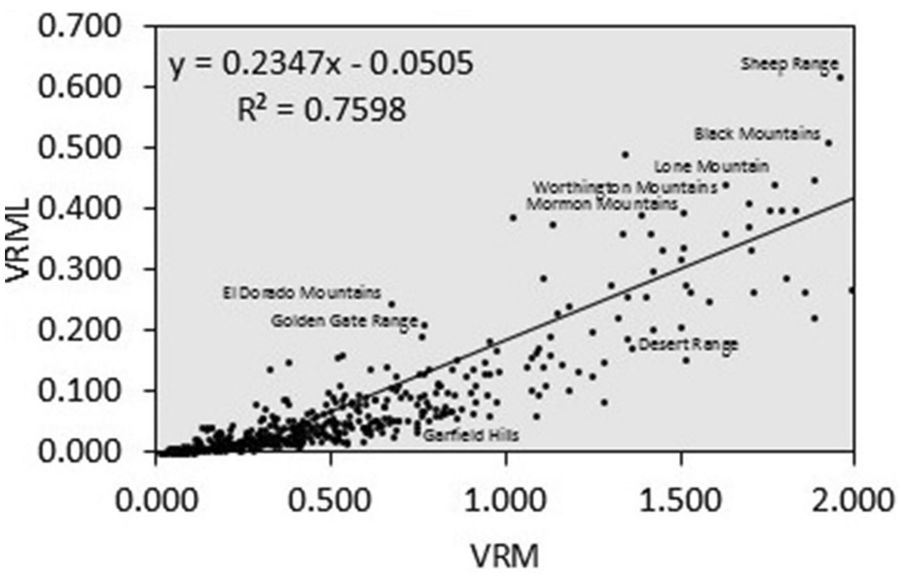

Fig. 3 Scatterplot of VRML predicted from VRM. Mountain ranges that are more rugged by VRML are shown above the best-fit line and mountains that are less rugged are below the line

mountain ranges had low values of VRM and VRML, yet the differences between VRM and VRML tended to increase with increasing ruggedness. According to both measures 79% of the top 10% most rugged mountain ranges in Nevada were located in the southern part of the state (Fig. 4A), but mountain ranges with large differences between the two ruggedness measures tended to be scattered throughout the state (Fig. 4B). Two mountain ranges, which showed the starkest contrast between VRM and VRML included the Sheep Range and the Desert Range, both adjacent mountain ranges located in southern Nevada just north of Las Vegas (Fig. 4C). In the Sheep Range VRML showed more extensive areas of high ruggedness (Fig. 4F) with the most rugged areas occurring in rocky outcrops and cliff bands (Fig. 4D). In contrast, the most rugged areas mapped by VRM were distributed along ridgelines and drainages (Fig. 4E). In the adjacent Desert Range areas mapped as rugged by VRM (Fig. 4H) and VRML (Fig. 4I) tended to be more similar to one another and tended to include a mix of ridgelines, drainages, mid-slope rock outcrops, and mid-slope erosional features (Fig. 4G). Finally, low ruggedness areas that were mapped as positive residuals are present in the northwestern and northcentral parts of Nevada Figs. 4A and 4B). Although these mountain ranges tend to have extensive flat-topped mesas they are also characterized by rim rock and deep canyons. It appears that VRML, by being able to better differentiate sharp versus smooth ridgelines, can better identify ruggedness in the form of sharp-edge rim rock and deep canyons. Considering a binary classification of rugged versus non-rugged terrain mid-slopes saw an increase in 59%, drainages a decrease in 45%, and ridges a decrease of 46% in the number of cells classified as high ruggedness (top 10%) when using VRML rather than VRM (Fig. 5).

Habitat selection by desert bighorn sheep during the parturition season

The spatial scales of the best models tended to be similar across ruggedness measures with models using finer-scale slope and medium to coarse-scale ruggedness performing the best. The most notable exception was for SAPR, in which coarser-scale slope and finer-scale ruggedness were more predictive (Fig. 6). All three modified ruggedness variables had similar patterns with scale and similar predictive power. The uncorrected versions of ACR and VRM had similar patterns with scale to one another. The single best model at Lone Mountain used ACRL at 810 m and slope at 150 m. In contrast, SAPR was most predictive in the coarsest-scale models of either slope or ruggedness but performed poorly when both variables were calculated at coarser scales. Modified versions of the ruggedness metrics (SAPRL, ACRL, VRML) tended to modestly improve habitat models relative to uncorrected version (SAPR, ACR, and

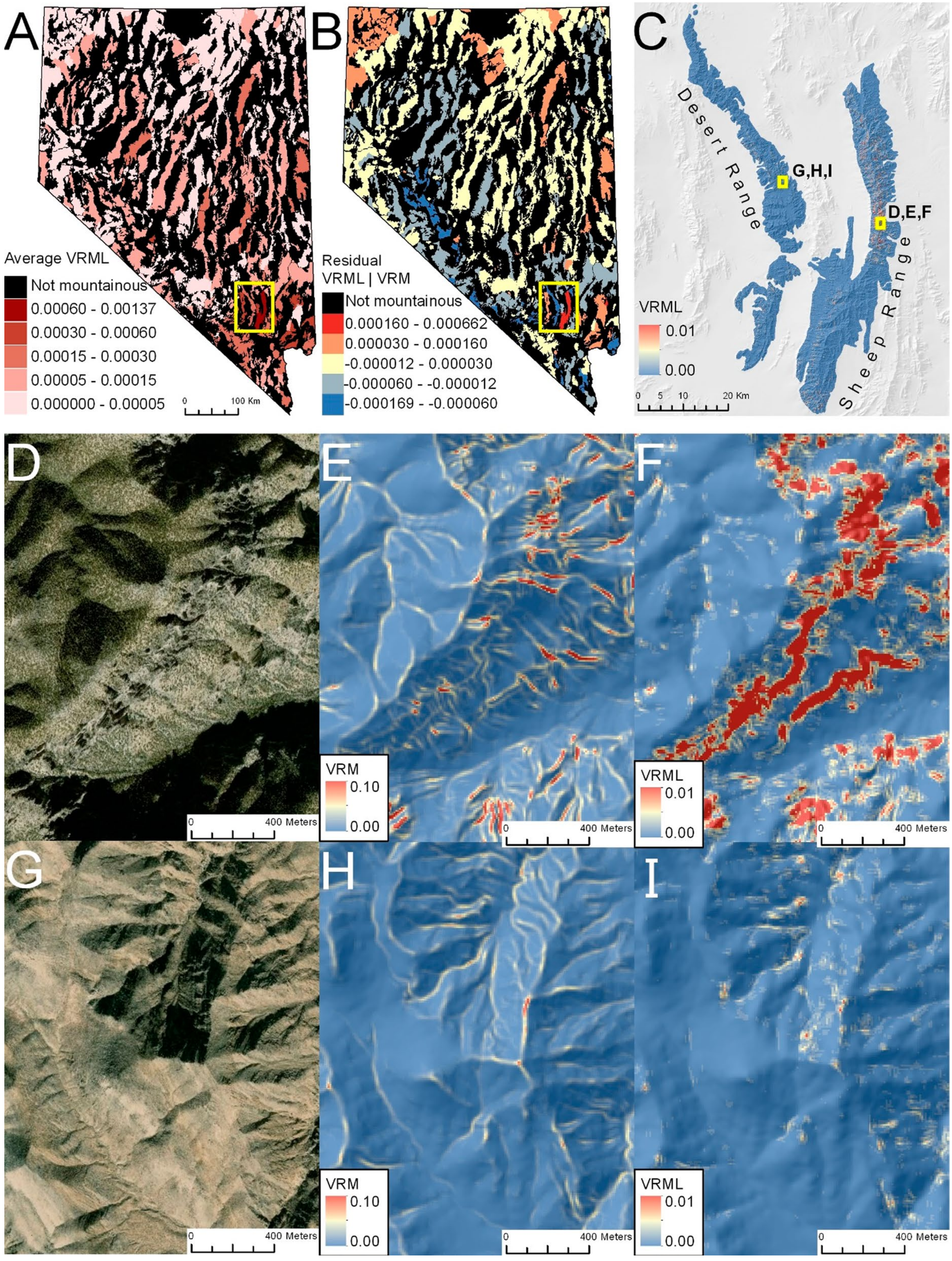
A
B
C
Average VRML
Not mountainous
0.00060 - 0.00137
0.00030 - 0.00060
0.00015 - 0.00030
0.00005 - 0.00015
0.000000 - 0.00005
0
100 Km
Residual
VRML | VRM
Not mountainous
0.000160 - 0.000662
0.000030 - 0.000160
-0.000012 - 0.000030
-0.000060 - -0.000012
-0.000169 - -0.000060
Desert Range
Sheep Range
G,H,I
D,E,F
VRML
0.01
0.00
0 5 10 20 Km
D
E
F
G
H
I
VRM
0.10
0.00
VRML
0.01
0.00
0
400 Meters

◂**Fig. 4** Results of the statewide analysis of vector ruggedness measure (VRM) and vector ruggedness measure local (VRML). **A** Map showing the average VRML for each of the 494 mountain ranges. Average VRML was 0.000075. **B** Map showing the residuals of VRML against VRM with red colors indicating that VRML was higher than expected and blues indicating that VRML was lower than expected. **C** Map showing the two focal mountain ranges: the Sheep Range and the Desert Range. Average VRML for the Sheep and Desert Ranges were 0.00061 and 0.00017 respectively suggesting that the Sheep Range is about 8.1 times more rugged than the average mountain range in Nevada and the Desert Range is 2.2 times more rugged than the average. The Sheep Range was the most rugged as measured by both VRM and VRML of the large mountain ranges in Nevada (> 6 km2) whereas the Desert Range was the 54th out of 494 mountain ranges. The residual VRML after accounting for VRM for the Sheep Range was 0.00021 and for the Desert Range was − 0.00010 making the Sheep Range the most positive residual of any large mountain range in Nevada and the Desert Range 479th out of 494. **D** Digital Globe Worldview 2 image dated 11/6/2018 showing a detailed view of the Sheep Range. **E** VRM with underlying hillshade for the detailed view of the Sheep Range. **F** VRML with underlying hillshade for the detailed view of the Sheep Range. **G** Digital Globe Worldview 2 image dated 11/11/2018 showing a detailed view of the Desert Range. **H** VRM with underlying hillshade for the detailed view of the Desert Range. **I** VRML with underlying hillshade for the detailed view of the Desert Range

VRM) as measured by the McFadden's pseudo- R2 (Fig. 6). At Lone Mountain the improvement in the models as measured by the difference in McFadden's R2 between the local and the regular for the best models was 0.027 for SAPR, 0.022 for ACR, and 0.020 for VRM (Fig. 6).

The slope of the ruggedness coefficient tended to increase as models were calculated at increasingly coarser spatial scales (Figure S1). Nevertheless, for models with slope at spatial scales less than 330 m, coefficients were highest at intermediate spatial scales (ruggedness 210—930). This pattern was most apparent in all three of the localized ruggedness measures. In contrast to ruggedness, finer-scale slope models tended to have higher slope coefficients (Figure S2). SAPR, but not SAPRL, tended to have coefficients in both ruggedness and slope that changed rapidly as models transitioned across the diagonal, perhaps resulting from correlations between slope and SAPR.

Selection coefficients for female bighorn sheep following parturition tended to be higher for ruggedness, and slightly lower for slope compared to females before parturition (Fig. 7). Both slope and ruggedness had credible intervals that were both positive and did not intersect zero (Fig. 7). Additionally, females selected areas on south facing slopes, closer to water, and with less tree cover, both pre and post parturition, although the degree of selection was different based on parturition period (Fig. 7). During both parturition periods, females also selected for areas with more bare ground, more perennial forbs and grasses, and higher shrub cover compared to females without dependent young (Fig. 7).

Discussion

The three components of the ideal ruggedness test represent three generations of topographic ruggedness measures (Table 1). The first generation of ruggedness measures pass the vertical distortion tests, but fail the other two tests, and should be thought of as representing variation in elevation rather than surface ruggedness. These measures, which included surface-area to planar-area ratio (SAPR) (Jenness 2004) as tested in this study, but also should include earlier ruggedness measures such as the Terrain Ruggedness Index (TRI) (Nelleman and Thomsen 1994; Riley et al. 1999) and the Land Surface Ruggedness Index (LSRI) (Beasom et al. 1983). Both the Arc-chord Ratio (Du Preez 2015) and the Vector Ruggedness Measure (Sappington et al. 2007) passed the vertical distortion and slope tests but failed the test that an ideal ruggedness measure not increase with the number of smooth folds. Hence, second generation ruggedness indices capture an important component in ruggedness, namely variation in aspect.

The localized versions of surface-area planar-area ratio (SAPR), arc-chord ratio (ACR), and vector ruggedness measure (VRM) passed all three tests. Furthermore, these localized ruggedness measures did a better job of mapping rugged terrain, such as rock outcrops and cliff bands, and allowed for the distinction between rugged ridgelines and drainages from smooth ridgelines and drainages. Although both the modified and uncorrected versions of the vector ruggedness measure were correlated with one another in this study we found that differences were large enough that rankings or comparisons among mountain ranges in Nevada might differ between the two versions. Although the concept of removing underlying smooth topographic variation for characterizing surface roughness is not completely novel

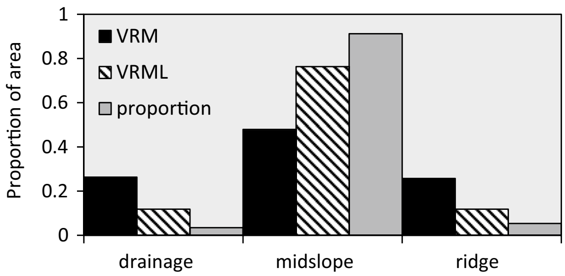

Fig. 5 Proportion of the highest 10% of VRM and VRML cells in three different topographic position categories: drainage, midslope, and ridgeline. The gray bars show the proportion of all cells in each of those topographic position categories without regard to the value of VRM or VRML

(Lindsay and Newman 2018), it has not yet been widely adopted in ecology. Adoption of this approach may lead to improved habitat models for species associated, positively or negatively, with rugged terrain.

The three components of landscape ruggedness may have different ecological interpretations. For example, first generation ruggedness indices representing variation in elevation may indicate areas that provide species with some ability to migrate in the face of climate change (Freeman et al. 2018). Areas with high, second generation ruggedness indices representing aspect diversity may indicate areas of high plant species richness resulting from the diversity of microclimates within a small geographic area (Ackerly et al. 2010). In addition, some of those areas may provide species with micro-refugia in the face of climate change. Third generation metrics represent localized surface roughness may represent undulations in the surface potentially indicating surface features such as boulder patches, which may be critical

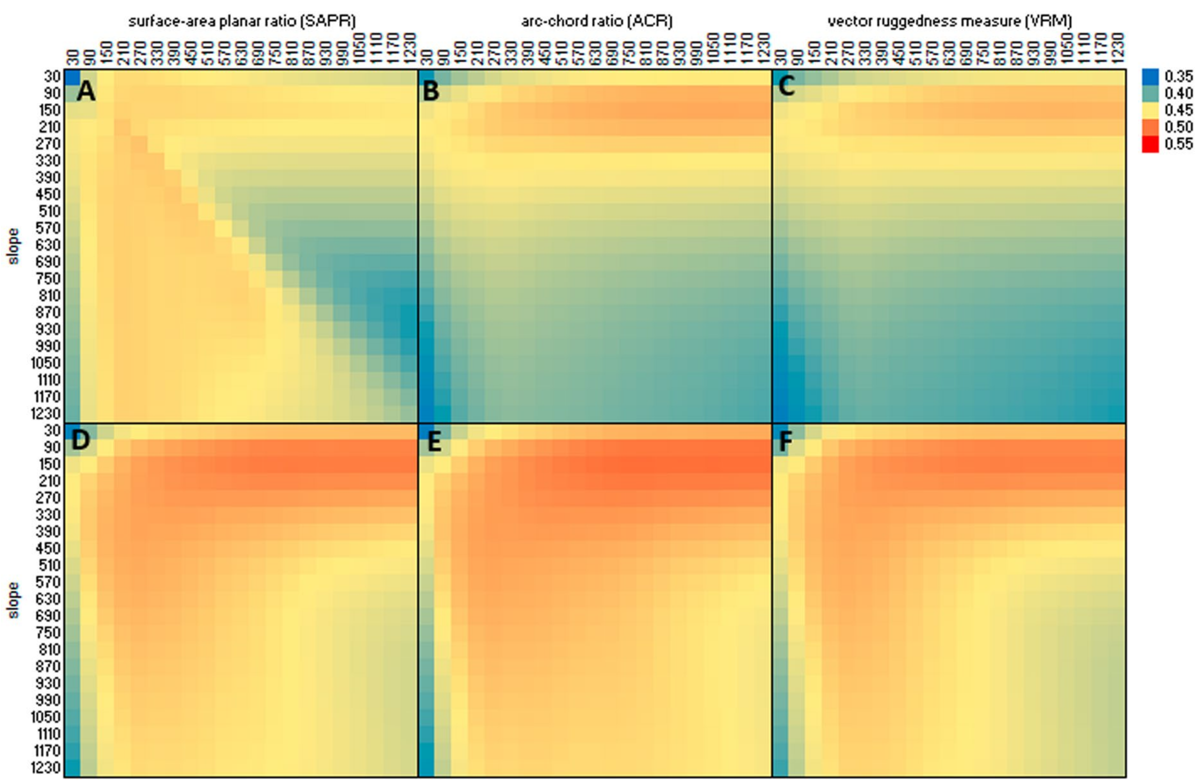

Fig. 6 McFadden's R2 for habitat selection functions for 1-month post-parturition female big horn sheep in the Lone Mountain study area. Models were tested across twenty-one spatial scales ranging from 30 to 1230 m for all scale combinations of ruggedness (columns) and slope (rows). The top row of models used the original **A** surface-area planar ratio, **B** arc-chord ratio, and **C** vector ruggedness without the modification used in this study. The bottom row used the novel local versions of **D** surface-area planar ratio, **E** arc-chord ratio, and **F** vector ruggedness with underlying topographic variation removed

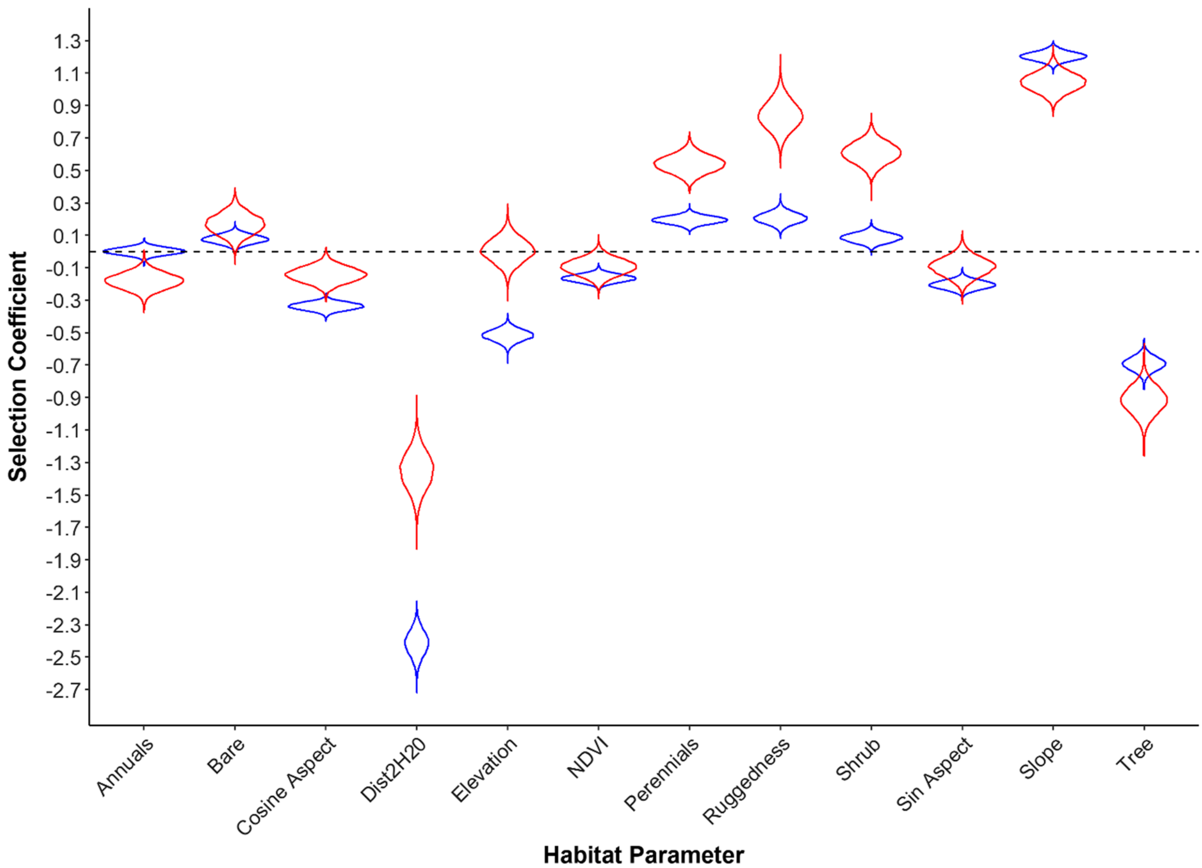

Fig. 7 Violin plots of density from the top Bayesian hierarchical model for habitat selection by desert bighorn sheep at Lone Mountain, Nevada (2016–2018). Blue density plots represent those estimated prior to parturition and red density plots represent those estimated post parturition (Blum et al. 2023a)

for certain species. For example, Gooley and Schauber (2022) found that rock crevices were the most important predictor for eastern woodrat (*Neotoma floridana*) population abundance in southern Illinois, USA. Improved mapping could potentially lead to the discovery of new sites for similar rock-obligate species. Metrics of localized surface roughness, such as VRM_L, ACR_L, and $SAPR_L$ used in this study, could be integrated directly into habitat models. Alternatively, these maps could be discretized and used to understand population processes under a metapopulation modeling approach (Wiens 1997). All three generations of ruggedness indices can be calculated as continuous variables from Digital Elevation Models, which is consistent with the adoption of surface metrics (McGarigal et al. 2009) and other continuous data for ecological analysis of landscapes.

Creating habitat models using multiple spatial scales is rapidly becoming more commonplace in ecology, and offers novel insights regarding how organisms interact with their environment (McGarigal et al. 2016). Topographic ruggedness and slope are both inherently scale-dependent variables; however, relatively few studies report the spatial scales at which these variables are calculated. Our results indicate that the best habitat models in our study area combined slope at fine, but not the finest, spatial scales, and ruggedness at moderate spatial scales, suggesting that this multi-scale model was both informative and more predictive than single-scale modeling. Variables calculated at broader spatial scales have been found to be more predictive for a range of wildlife taxa (Weisberg et al. 2014; Zeller et al. 2017), however the most predictive scale is related to the behavioral ecology of the species of interest, as well as the unique combination of habitat features present within a particular study area. Female desert bighorn sheep with young at Lone Mountain, Nevada selected coarse scales of ruggedness (810 m) and fine scales of slope (150 m). Ruggedness may have been selected at coarse spatial scales because concealment from predators is very important for dependent young in the 1st month of life and coarser scales of ruggedness may be more related to viewsheds and concealment. In contrast, steeper terrain may have been selected because it provides opportunities for desert bighorn sheep to escape from predators (Berger 1991). The new approach outlined in this paper isolates the effect of fine-scale variation in the z-dimension from more generalized effects of variation in slope and aspect, and therefore facilitates the functional interpretation of predictor variables used in a habitat model. Because the meaning of topographic roughness becomes more specific and less confounded with other components of habitat, ecological relationships can be more readily inferred.

Conclusion

In this paper we provide an approach that can be used to modify a wide range of topographic ruggedness measures. We also introduced the idea of three generations of ruggedness indices representing elevation variability, aspect diversity, and fine-scale surface ruggedness. We present and test an "ideal ruggedness test", in which only our localized ruggedness measures passes all three criteria. Adoption of modified ruggedness measures will likely help diminish confusion between ridgelines and drainages with rugged terrain. Nevertheless, the other two aspects of ruggedness (elevation variability and aspect diversity) may be equally, or more important, for many ecological applications. Moving forward, users should be explicit about the particular metrics they use as the three generations of metrics represent different aspects of topographic ruggedness. Specifically referring to ruggedness metrics as elevation variability, aspect diversity, and local surface ruggedness may help illuminate which particular functional role that ruggedness represents. Researchers should also consider both ruggedness and slope at different spatial scales since the smallest scale may not always be the most informative. Finally, it is critical to consider the ecological processes that are likely to be affected by topographic ruggedness, as in our case study in which ruggedness appears to reflect habitat concealment whereas slope represents escape terrain.

Acknowledgements We would like to acknowledge the Nevada Department of Wildlife and the Agricultural Experiment Station at the University of Nevada, Reno for support of this project.

Author contributions TED and PJW were responsible for the study conception. All authors contributed to the study design and edits throughout the writing process. MEB conducted field work. TED and MEB performed data analysis. KM and MEB obtained funding and oversaw the bighorn sheep portion of the manuscript.

Funding Agricultural Experiment Station at the University of Nevada, Reno. Nevada Department of Wildlife, Agricultural Experiment Station at the University of Nevada, Reno

Data availability The datasets generated or analyzed during the current study are available from the corresponding author on reasonable request.

Code availability All code used for this study will be made available upon reasonable request.

Declarations

Conflict of interest The authors have no conflicts of interest to disclose.

Ethical approval This research was conducted in compliance with Scientific Collection Permits from the states of Nevada, California, and Oregon, and under oversight of the University of Nevada Reno's Animal Care and Use Committee.

Consent to participate Not applicable.

Consent for publication Not applicable

References

Ackerly DD, Loarie SR, Cornwell WK, Weiss SB, Hamilton H, Branciforte R, Kraft NJB (2010) The geography of climate change: implications for conservation biogeography. Divers Distrib 16:476–487

Amatulli G, Domisch S, Tuanmu MN, Parmentier B, Ranipeta A, Malczyk J, Jetz W (2018) A suite of global, cross-scale topographic variables for environmental and biodiversity modeling. Scientific Data 5:1–15

Austin MP (2002) Spatial prediction of species distribution: an interface between ecological theory and statistical modelling. Ecol Model 157:101–118

Baker WL, Weisberg PJ (1995) Landscape analysis of the forest-tundra ecotone in Rocky Mountain National Park, Colorado. Prof Geogr 47:361–375

Bates D, Maechler M, Bolker B, Walker S (2015) Fitting linear mixed-effects models using lme4. J Stat Softw 67:1–48

Beasom SL, Wiggers EP, Giardino JR (1983) A technique for assessing land surface ruggedness. J Wildl Manag 47:1163–1166

Berger J (1991) Pregnancy incentives, predation constraints and habitat shifts: experimental and field evidence for wild bighorn sheep. Anim Behav 41:61–77

Bishop CJ, Freddy DJ, White GC, Stephenson TR, Wolfe LL, Watkins BE (2007) Using vaginal implant transmitters to aid in capture of mule deer dependent young. J Wildl Manag 71:945–954

Bleyhl B, Arakelyan M, Askerov E, Bluhm H, Gavashelishvili A, Ghasabian M, Ghoddousi A, Heidelberg A, Khorozyan I, Malkhasyan A, Manvelyan K, Masoud M, Moqanaki EM, Radeloff VC, Soofi M, Weinberg P, Zazanashvili N, Kuemmerle T (2019) Assessing niche overlap between domestic and threatened wild sheep to identify conservation priority areas. Divers Distrib 25:129–141

Blum ME, Stewart KM, Shoemaker KT, Cox M, Wakeling BF, Dilts TE, Bennett JR, Bleich VC (2023). Changes in selection of resources with reproductive state in a montane ungulate. Mov. Ecol. https://doi.org/10.1186/s40462-023-00378-1

Blum ME, Stewart KM, Cox M, Shoemaker KT, Bennett JR, Sullivan BW, Wakeling BF, Bleich VC (2023a). Variation in diet of desert bighorn sheep (Ovis canadensis nelsoni): Tradeoffs associated with parturition. Front. Ecol. Evol. 10: e1071771.

Blum ME, Stewart KM, Shoemaker KT, Cox M, Wakeling BF, Dilts TE, Bennett JR, Bleich VC (2023b). Changes in selection of resources with reproductive state in a montane ungulate. Mov. Ecol. https://doi.org/10.1186/s40462-023-00378-1

Buechner HK (1960) The bighorn sheep in the United States, its past, present, and future. Wildl Monogr 4:3–174

Buffington JM, Montgomery DR, Greenberg HM (2004) Basin-scale availability of salmonid spawning gravel as influenced by channel type and hydraulic roughness in mountain catchments. Can J Fish Aquat Sci 61:2085–2096

Burt TP, Butcher DP (1985) Topographic controls of soil moisture distributions. J Soil Sci 36:469–486

Chetkiewicz CLB, Boyce MS (2009) Use of habitat selection functions to identify conservation corridors. J Appl Ecol 46:1036–1047

Copeland SM, Harrison SP (2015) Identifying plant traits associated with topographic contrasts in a rugged and diverse region (Klamath-Siskiyou Mts, OR, USA). Ecography 38:569–577

Dobrowski SZ, Abatzoglou JT, Greenberg JA, Schladow SG (2009) How much influence does landscape-scale physiography have on air temperature in a mountain environment? Agric for Meteorol 149:1751–1758

Donadio E, Buskirk SW (2016) Linking predation risk, ungulate antipredator responses, and patterns of vegetation in the high Andes. J Mammal 97:966–977

Freeman BG, Scholer MN, Ruiz-Gutierrez V, Fitzpatrick JW (2018) Climate change causes upslope shifts and mountaintop extirpations in a tropical bird community. Proc Natl Acad Sci 115:11982–11987

Gooley AC, Schauber EM (2022) Trees, owls, worms, and crevices: which habitat factors predict local woodrat demographics? J Mammal 103:970–978

Graham NAJ, Nash KL (2013) The importance of structural complexity in coral reef ecosystems. Coral Reefs 32:315–326

Heffelfinger LJ, Stewart KM, Shoemaker KT, Darby NW, Bleich VC (2020) Balancing current and future reproductive investment: variation in resource selection during stages of reproduction in a long-lived herbivore. Front Ecol Evol 8:163

Hobson RD (1972) Surface Roughness in Topography: A Quantitative Approach. In: Chorley RJ (ed) Spatial Analysis in Geomorphology. Methuen & Co., London, pp 221–245

Hoglander C, Dickson BG, Rosenstock SS, Anderson JJ (2015) Landscape models of space use by desert bighorn sheep in the sonoran desert of Southwestern Arizona. J Wildl Manag 79:77–91

Jahner JP, Matocq MD, Malaney JL, Cox M, Wolff P, Gritts MA, Parchman TL (2019) The genetic legacy of 50 years of desert bighorn sheep translocations. Evol Appl 12:198–213

Jenness JS (2004) Calculating landscape surface area from digital elevation models. Wildl Soc Bull 32:829–839

Johnson CJ, Nielsen SE, Merrill EH, McDonald TL, Boyce MS (2006) Habitat selection functions based on use-availability data: theoretical motivation and evaluation methods. J Wildl Manag 70:347–357

Johnson HE, Hebblewhite M, Stephenson TR, German DW, Pierce BM, Bleich VC (2013) Evaluating apparent competition in limiting the recovery of an endangered ungulate. Oecologia 171:295–307

Jones MO, Allred BW, Naugle DE, Maestas JD, Donnelly P, Metz LJ, Karl JW, Smith R, Bestelmeyer BT, Boyd CS, Kerby JD, McIver JD (2018) Innovation in rangeland monitoring: annual, 30 m, plant functional type percent cover maps for US rangelands, 1984–2017. Ecosphere 9:e02430

Kellner K (2019) jagsUI: A wrapper around ‘rjags’ to streamline ‘JAGS’ analyses. R package version 1.5.1. https://CRAN.R-project.org/package=jagsUI

Krawchuk MA, Haire SL, Coop J, Parisien MA, Whitman E, Chong G, Miller C (2016) Topographic and fire weather controls of fire refugia in forested ecosystems of northwestern North America. Ecosphere 7:e01632

Kunkel KE, Atwood TC, Ruth TK, Pletscher DH, Hornocker MG (2013) Assessing wolves and cougars as conservation surrogates. Anim Conserv 16:32–40

Leempoel K, Parisod C, Geiser C, Daprà L, Vittoz P, Joost S (2015) Very high-resolution digital elevation models: are multi-scale derived variables ecologically relevant? Methods Ecol Evol 6:1373–1383

Li H, Reynolds JF (1995) On definition and quantification of heterogeneity. Oikos 73:280–284

Lindsay JB, Newman DR (2018) Hyper-scale analysis of surface roughness. PeerJ Preprints 6:e27110v1

Lone K, Loe LE, Gobakken T, Linnell JD, Odden J, Remmen J, Mysterud A (2014) Living and dying in a multi-predator landscape of fear: roe deer are squeezed by contrasting pattern of predation risk imposed by lynx and humans. Oikos 123:641–651

Macdonald DW, Bothwell HM, Hearn AJ, Cheyne SM, Haidir I, Hunter LT, Kaszta Ż, Linkie M, Macdonald EA, Ross J, Cushman SA (2018) Multi-scale habitat selection modeling identifies threats and conservation opportunities for the Sunda clouded leopard (Neofelis diardi). Biol Cons 227:92–103

Manly BFL, McDonald LL, Thomas DL, MacDonald TL, Erickson WP (2002) Resource selection by animals: statistical design and analysis for field studies. Kluwer Academic, London, UK

McCann LJ (1956) Ecology of the mountain sheep. Am Midl Nat 56:297–324

McFadden D (1974) Conditional logit analysis of qualitative choice behavior. In: Zarembka P (ed) Frontiers in economics. Academic Press, New York, pp 105–142

McGarigal K, Tagil S, Cushman SA (2009) Surface metrics: an alternative to patch metrics for the quantification of landscape structure. Landscape Ecol 24:433–450

McGarigal K, Wan HY, Zeller KA, Timm BC, Cushman SA (2016) Multi-scale habitat selection modeling: a review and outlook. Landscape Ecol 31:1161–1175

Melton MA (1958) Correlation structure of morphometric properties of drainage systems and their controlling agents. J Geol 66:442–460

Monteith KL, Hayes MM, Kauffman MJ, Copeland HE, Sawyer H (2018) Functional attributes of ungulate migration: landscape features facilitate movement and access to forage. Ecol Appl 28:2153–2164

Pickett ST, Cadenasso ML (1995) Landscape ecology: spatial heterogeneity in ecological systems. Science 269:331–334

Du Preez C (2015) A new arc–chord ratio (ACR) rugosity index for quantifying three-dimensional landscape structural complexity. Landscape Ecol 30:181–192

Rengstorf AM, Yesson C, Brown C, Grehan AJ (2013) High resolution habitat suitability modelling can improve conservation of vulnerable marine ecosystems in the deep sea. J Biogeogr 40:1702–1714

Riley SJ, DeGloria SD, Elliot R (1999) Index that quantifies topographic heterogeneity. Intermount J Sci 5:23–27

Sappington JM, Longshore KM, Thompson DB (2007) Quantifying landscape ruggedness for animal habitat analysis: a case study using bighorn sheep in the Mojave Desert. J Wildl Manag 71:1419–1426

Seidel DP, Boyce MS (2015) Patch-use dynamics by a large herbivore. Mov Ecol 3:1–10

Smith JB, Grovenburg TW, Jenks JA (2015) Parturition and bed site selection of bighorn sheep at local and landscape scales. J Wildl Manag 79:393–401

Strahler AN (1954) Quantitative geomorphology of erosional landscapes: Comptes Rendus, 19th Session, International Geological Congress, Algiers, Sec. XIII, pp 341–354

US Geological Survey (2009) National Elevation Dataset. http://ned.usgs.gov/. Accessed 12 November 2019.

Walbridge S, Slocum N, Pobuda M, Wright DJ (2018) Unified geomorphological analysis workflows with Benthic Terrain Modeler. Geosciences 8:94

Weisberg PJ, Dilts TE, Becker ME, Young JS, Wong-Kone DC, Newton WE, Ammon EM (2014) Guild-specific responses of avian species richness to lidar-derived habitat heterogeneity. Acta Oecologica 59:72–83

Weiss A (2001). Topographic position and landforms analysis. In: ESRI user conference, San Diego, CA.

Whitehouse DJ (1994) Handbook of Surface Metrology. CRC Press

Wiens JA (1997) Metapopulation dynamics and landscape ecology. In: Hanski I, Gilpin M (eds) Metapopulation biology. Academic Press, Cambridge, MA, pp 43–62

Wiens JA, Stenseth NC, Van Horne B, Ims RA (1993) Ecological mechanisms and landscape ecology. Oikos 66:369–380

Yang J, Weisberg PJ, Dilts TE, Loudermilk EL, Scheller RM, Stanton A, Skinner C (2015) Predicting wildfire occurrence distribution with spatial point process models and its uncertainty assessment: a case study in the lake Tahoe Basin. USA. Int J Wildland Fire 24:380–390

Zeller KA, Vickers TW, Ernest HB, Boyce WM (2017) Multilevel, multi-scale habitat selection functions and resistance surfaces for conservation planning: Pumas as a case study. PLoS ONE 12:e0179570